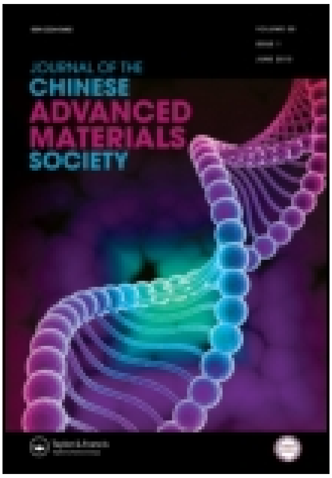

Journal of the Chinese Advanced Materials Society
Publication details, including instructions for authors and subscription information:
http://www.tandfonline.com/loi/tadm20

Graphite nanoplatelets and/or barium titanate/polymer nanocomposites: fabrication, thermomechanical properties, dielectric response and energy storage

A.C. Patsidis[ab], K. Kalaitzidou[ac], D.L. Anastassopoulos[d], A.A. Vradis[d] & G.C. Psarras[b]
[a] School of Mechanical Engineering, Georgia Institute of Technology, Atlanta, GA, USA
[b] Department of Materials Science, University of Patras, Patras, Greece
[c] School of Materials Science and Engineering, Georgia Institute of Technology, Atlanta, GA, USA
[d] Department of Physics, University of Patras, Patras, Greece

To cite this article: A.C. Patsidis, K. Kalaitzidou, D.L. Anastassopoulos, A.A. Vradis & G.C. Psarras (2014) Graphite nanoplatelets and/or barium titanate/polymer nanocomposites: fabrication, thermomechanical properties, dielectric response and energy storage, Journal of the Chinese Advanced Materials Society, 2:3, 207-221, DOI: 10.1080/22243682.2014.937742

To link to this article: http://dx.doi.org/10.1080/22243682.2014.937742

Journal of the Chinese Advanced Materials Society, 2014
Vol. 2, No. 3, 207–221, http://dx.doi.org/10.1080/22243682.2014.937742

Graphite nanoplatelets and/or barium titanate/polymer nanocomposites: fabrication, thermomechanical properties, dielectric response and energy storage

A.C. Patsidis[a,b], K. Kalaitzidou[a,c], D.L. Anastassopoulos[d], A.A. Vradis[d] and G.C. Psarras[b]*

[a]*School of Mechanical Engineering, Georgia Institute of Technology, Atlanta, GA, USA;* [b]*Department of Materials Science, University of Patras, Patras, Greece;* [c]*School of Materials Science and Engineering, Georgia Institute of Technology, Atlanta, GA, USA;* [d]*Department of Physics, University of Patras, Patras, Greece*

(*Received 14 May 2014; revised 18 June 2014; accepted 18 June 2014*)

Epoxy composites reinforced with (1) micro-size barium titanate ($BaTiO_3$), (2) nano-size $BaTiO_3$, (3) graphite nanoplatelets (GNP), (4) combination of micro and nano $BaTiO_3$ and (5) combination of $BaTiO_3$ and GNP were fabricated and studied, in terms of the type, size and amount of the filler content. Scanning electron microscopy and X-ray diffraction spectra were employed for the investigation of the systems' morphology. Dynamic mechanical analysis, static mechanical tests and broadband dielectric spectroscopy were used in order to study the properties of the produced systems. Reinforced systems exhibit higher values of storage modulus and dielectric permittivity compared to neat epoxy. Dielectric spectra reveal the presence of two relaxation processes arising from the glass to rubber transition of the polymer matrix (α-mode), and the re-orientation of polar side groups of the polymer chains (β-mode). Finally, the energy storage efficiency of the prepared composite systems was examined in terms of the energy density as a function of the temperature, frequency, type, size and amount of the employed filler.

Keywords: exfoliated graphite nanoplatelets; barium titanate; polymer nanocomposites; dielectric properties; thermomechanical properties; energy storage

1. Introduction

The scientific and technological impact of nanostructured materials is well established and appreciated nowadays, because of the improvement in thermomechanical properties, flame resistance, electrical properties, etc. and the resulting potential for numerous applications. Nanodielectrics represent a specific category of nanomaterials, which includes polycrystalline semiconducting or insulating materials, with grain diameter at the nanoscale level and polymer composites incorporating nanoinclusions.[1] Polymer nanocomposites exhibit a number of advantages, such as easy processing and thermomechanical stability, resistance to corrosive environments, etc. Moreover their dielectric behaviour can be tailored by simply controlling the type, size and amount of the nanofiller. Thus, polymer nanocomposites are expected to replace conventional insulating materials in a variety of applications. Current applications of inorganic filler–polymer matrix nanocomposites include packaging, electromagnetic radiation shielding, circuit board, interlayer dielectrics, leakage current controllers, self-current regulators, passive protection, etc.[2–4]

---

*Corresponding author. Email: G.C.Psarras@upatras.gr

Nanodielectrics associate dielectrics with nanotechnology; further nanoinclusions could be able to serve as an inherent network of nanocapacitors. Charging and discharging under control, nanocapacitors, embedded in a matrix, define an energy-storing procedure at the nanoscale level, introducing thus a new type of nanodevice. The latter could be used in emerging technological applications such as cellular phones, wireless personal digital assistants, acoustic emission sensors, stationary power systems and hybrid electric vehicles.[2–5]

Embedding piezoelectric or ferroelectric particles within a polymer matrix induces functionality to the resulting composite because of the variable polarization of the inclusions.[5–7] The stress- or temperature-induced variations of polarization is directly reflected to the composite's dielectric permittivity. Especially in the case of ferroelectric inclusions, the "disorder-to-order" structural transition of the filler or, in other words, the transition from the polar ferroelectric phase to the non-polar paraelectric phase at the critical Curie temperature provides a suitable base for the development of a smart materials system.[5,8,9] Materials systems, which are able to vary some of their properties in a controllable and reversible manner, when triggered by an external stimulus, are referred as smart materials.[10–12]

The goal of this study was to develop lightweight, easy-to-make, low-cost dielectric materials able to store energy and harvest it with minimum losses, and with appropriate mechanical performance. For this reason, different series of composite materials were fabricated and studied. In particular, the following composite systems were prepared: $BaTiO_3$ microparticles/epoxy composites, $BaTiO_3$ nanoparticles/epoxy composites, exfoliated graphite nanoplatelets (GNP)/epoxy composites, and hybrid systems of epoxy with both types of $BaTiO_3$ particles (micro and nano) and hybrids of epoxy incorporating at the same time $BaTiO_3$ nanoparticles and GNP, varying each time the amount of the employed filler content. Morphology, viscoelastic properties, static mechanical behaviour and dielectric response of all systems were investigated by means of scanning electron microscopy (SEM) and X-ray diffraction (XRD), dynamic mechanical analysis (DMA), flexural tests and broadband dielectric spectroscopy (BDS). The determined properties between $BaTiO_3$/epoxy, GNP/epoxy and $BaTiO_3$/GNP/epoxy hybrid composites were compared in order to provide an understanding of the structure–properties relationships and to specify the optimum amount and filler type. Finally, the energy density of all studied systems was calculated, targeting to investigate the energy storage efficiency of the prepared composites.

2. Experimental

2.1. Materials

Composite systems were fabricated by employing commercially available materials. In particular, compounds with the trade name Araldite LY 564 (a low viscosity epoxy resin) and Aradur-HY2954 (cycloaliphatic polyamine), both supplied by Huntsman Advanced Materials (Switzerland), were used as a prepolymer and a curing agent, respectively. Micro- and nano-$BaTiO_3$ particles, supplied by Sigma Aldrich (Taufkirchen, Germany), with a mean particle diameter of 2 μm and 30–50 nm, respectively, were used. GNP with a mean particle diameter less than 1 μm and an average thickness of 10–20 nm were supplied by XG Sciences (East Lansing, MI).

2.2. Specimens fabrication

Composites were fabricated via the solution method. The nano-filler powder ($BaTiO_3$ or GNP) was mixed with isopropyl alcohol (IPA) for 40 minutes at ambient temperature, using a sonication probe (1/2″ probe size, 40% amplitude for 40 minutes, Misonix 4000) in order to break down the fillers' agglomerates. After filtering the IPA, the powder was collected. An appropriate filler amount was dispersed, at ambient temperature, in epoxy using a magnetic stirring plate at 800 rpm for one hour and at the temperature of $T = 60$ °C. The curing agent was then added to the filler/monomer solution at a 35/100 wt/wt ratio, and the mixing was continued at ambient temperature for 30 minutes at 800 rpm. The mixture was degassed in a vacuum oven, and cast in moulds. Initial polymerization (curing) was conducted at $T = 80$ °C for one hour, followed by post-curing at $T = 100$ °C for four hours. The filler content varied between 3 and 10 phr (parts per hundred resin per weight) in the case of nano-$BaTiO_3$ and GNP composites, and between 7 and 20 phr in the case of micro-$BaTiO_3$ composites.

2.3. Composites characterization

The morphology of the composites was investigated by employing a Zeiss Ultra 60 SEM device, while XRD spectra were taken via a Philips PW 1050/25 goniometer and a Cu Kα X-ray tube ($\lambda = 1.5418$ Å). Details of the XRD tests are given elsewhere.[13] Specimens were checked for the presence of voids and agglomerates, and the achieved dispersion of fillers within the polymer matrix. Viscoelastic properties, such as storage and loss modulus and tan delta, of the composites were studied using DMAQ800 by TA Instruments (Lukens Drive, New Castle, U.S.A.). The employed technique was single-cantilever mode applying a force of 100 mN, at a constant frequency of 1 Hz, as a function of temperature. Temperature was varied from 30 °C to 160 °C, at a heating rate of 5 °C/min. Flexural modulus and strength were measured according to the ASTM D790 specification.

Composites' dielectric response was assessed via BDS using an alpha-N frequency response analyser and a 1200 BDS dielectric cell provided by Novocontrol Technologies (Hundsagen, Germany). Isothermal frequency scans were conducted, for each specimen, from ambient temperature to 160 °C in steps of 5 °C, in the frequency range 0.1 Hz to 10 MHz. Temperature was varied with a Novotherm system supplied also by Novocontrol Technologies. Specimens were placed between two gold-plated electrodes, the applied amplitude of voltage was kept constant at 1 V, the dielectric cell was electrically shielded in order to avoid measuring any stray capacitance, and data acquisition was conducted, in real time, with Win Data software of Novocontrol Technologies.

3. Results and discussion

Representative SEM micrographs of the hybrid composite systems are shown in Figure 1. SEM images reveal that $BaTiO_3$ and GNP nanoinclusions are dispersed within the whole polymer matrix without exhibiting any preferential distribution, although nanodispersions coexist with small agglomerates in all studied systems. Figure 2 depicts the XRD spectra of the (i) 7 phr nano-$BaTiO_3$/3 phr micro-$BaTiO_3$/epoxy, (ii) 3 phr nano-$BaTiO_3$/7 phr micro-$BaTiO_3$/epoxy, (iii) 7 phr nano-$BaTiO_3$/3 phr GNP/epoxy and (iv) 3 phr nano-$BaTiO_3$/7 phr GNP/epoxy systems, while the inset shows the XRD spectrum of the 10 phr GNP/epoxy nanocomposite. Recorded peaks are characteristic for both $BaTiO_3$ (micro and nano) types, and for GNP. Spectra from specimens with GNP include the graphite-like (002) peak located at 26.5°, which is present in the diffractograms of different allotropic forms of carbon.[13–16] XRD patterns of $BaTiO_3$-containing samples exhibit the characteristic peaks of (100), (101), (111), (002) and (200) located at 22.0°, 31.4°, 38.7°, 45.0° and 45.3°, respectively.[17] It should be noted that the spectrum of

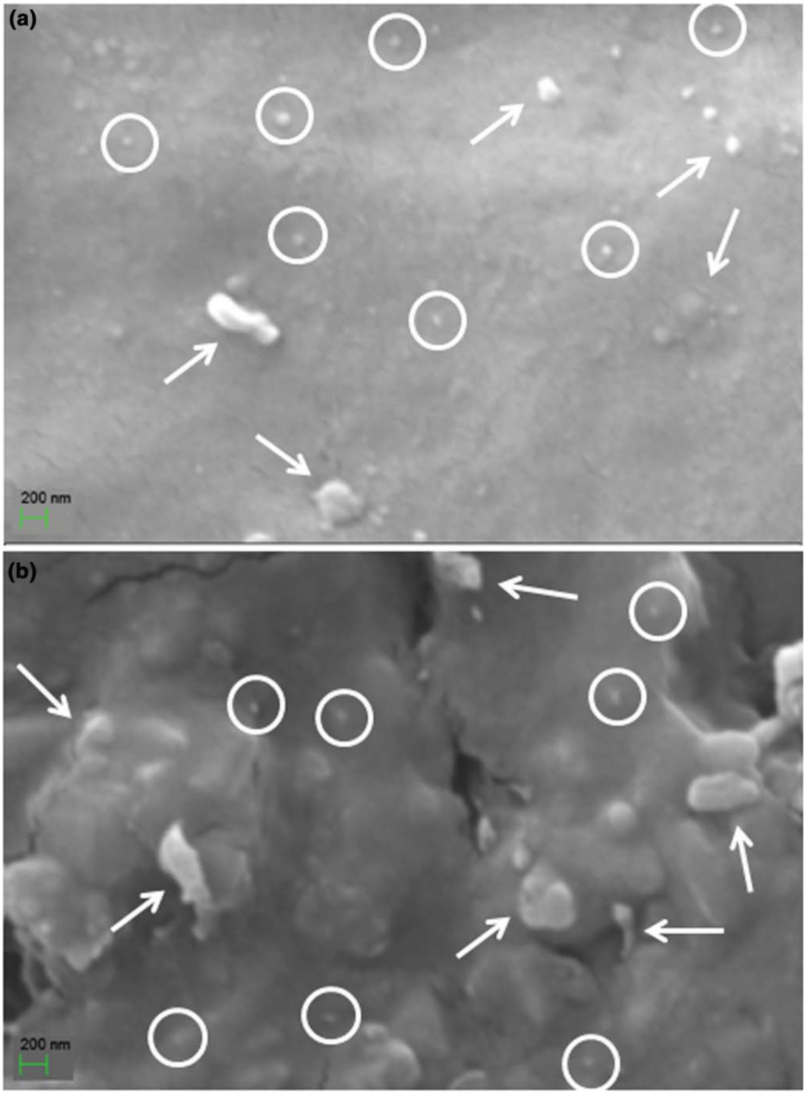

Figure 1. SEM images from the hybrid specimens with: (a) 3 phr $BaTiO_3$/7 phr GNP and (b) 7 phr $BaTiO_3$/3 phr GNP inclusions. Circles indicate the presence of $BaTiO_3$ nanoparticles, while arrows indicate the presence of GNP.

Figure 2(ii), representing the composite with maximum loading in micro-$BaTiO_3$ particles, exhibits the (002) and (200) reflections, which are considered as the fingerprint of the pure tetragonal structure of micro-$BaTiO_3$ particles.[8,9] Spectra from systems containing only nano-$BaTiO_3$ particles exhibit only the (200) peak, indicating that the cubic-like structure is dominant in their case.[8,9] Furthermore, the two wide peaks in the vicinity of 7^o and 18^o that are present in all spectra are related to the amorphous epoxy matrix.

Viscoelastic properties of all the examined composites are depicted in Figures 3 and 4. Figure 3(a) presents the variation of storage modulus as a function of temperature varying the filler content for the GNP/epoxy and $BaTiO_3$/epoxy nanocomposites, while the inset

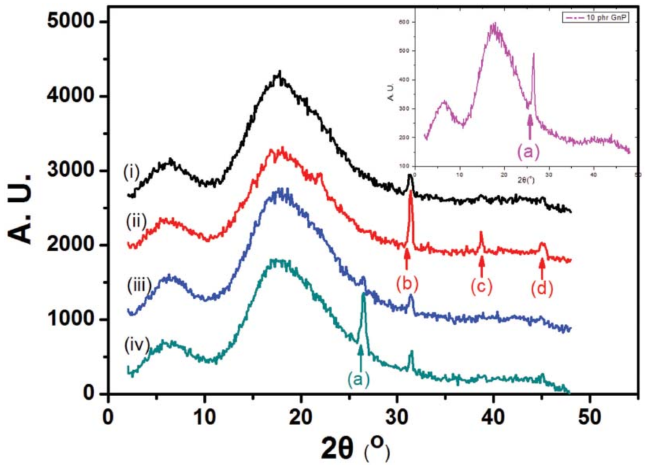

Figure 2. XRD diffractograms of the (i) 7 phr nano-$BaTiO_3$/3 phr micro-$BaTiO_3$/epoxy, (ii) 3 phr nano-$BaTiO_3$/7 phr micro-$BaTiO_3$/epoxy, (iii) 7 phr nano-$BaTiO_3$/3 phr GNP/epoxy and (iv) 3 phr nano-$BaTiO_3$/7 phr GNP/epoxy systems. Inset presents the spectrum of the 10 phr GNP/epoxy nanocomposite. Arrow lines indicate peaks positions for: (a) graphite-like peak, and (b), (c) and (d) $BaTiO_3$ peaks.

depicts storage modulus versus temperature for the 3 phr $BaTiO_3$/7 phr GNP/epoxy and 7 phr $BaTiO_3$/3 phr GNP/epoxy hybrid systems. Glass-to-rubber transition becomes evident, in all studied systems, via the abrupt decrease of the storage modulus values. At temperatures below the glass-to-rubber transition area, composite systems exhibit higher values of storage modulus, which increase systematically with filler content in both types of nanocomposites. Considering the nanocomposites with equal $BaTiO_3$ or GNP content, the GNP/epoxy resin composites exhibit higher values of storage modulus, and optimum viscoelastic performance is demonstrated by the composite with the highest GNP content, that is, the 10 phr GNP/epoxy specimen. Hybrid systems in the inset of Figure 3(a) follow the same behaviour. Although the total filler content is constant at 10 phr, the specimen with the higher GNP concentration exhibits the enhanced values of storage modulus.

At temperatures above 100 °C, the transition from the rigid glassy state to the softer rubbery state is accompanied by dissipation of energy, which becomes apparent from the recorded loss peaks in Figure 3(b). Glass transition temperature (T_g) can be determined via the loss peak abscissa. Neglecting small variations from system to system, which possibly reflects the microstructure of each specimen, T_g appears not to be affected by the amount and the type of the filler content, being in the vicinity of 130 °C. In general, T_g seems not to be dependent on the filler content, which is in accordance with results obtained via differential calorimetry studies reported earlier.[18] Besides the general trend, the glass transition temperature of hybrid nanocomposites, containing both $BaTiO_3$ and GNP inclusions (inset of Figure 3(b)) and the 3 phr GNP/epoxy specimen, deviates from the corresponding value of pure epoxy. Although further investigation is needed, these deviations in T_g values could be ascribed to the occurring interactions between filler and matrix.

The viscoelastic response of micro- and nano-$BaTiO_3$/epoxy composites is shown in Figure 4, while the inset depicts the viscoelastic properties of the 3 phr nano-$BaTiO_3$/7 phr micro-$BaTiO_3$/epoxy and 7 phr nano-$BaTiO_3$/3 phr

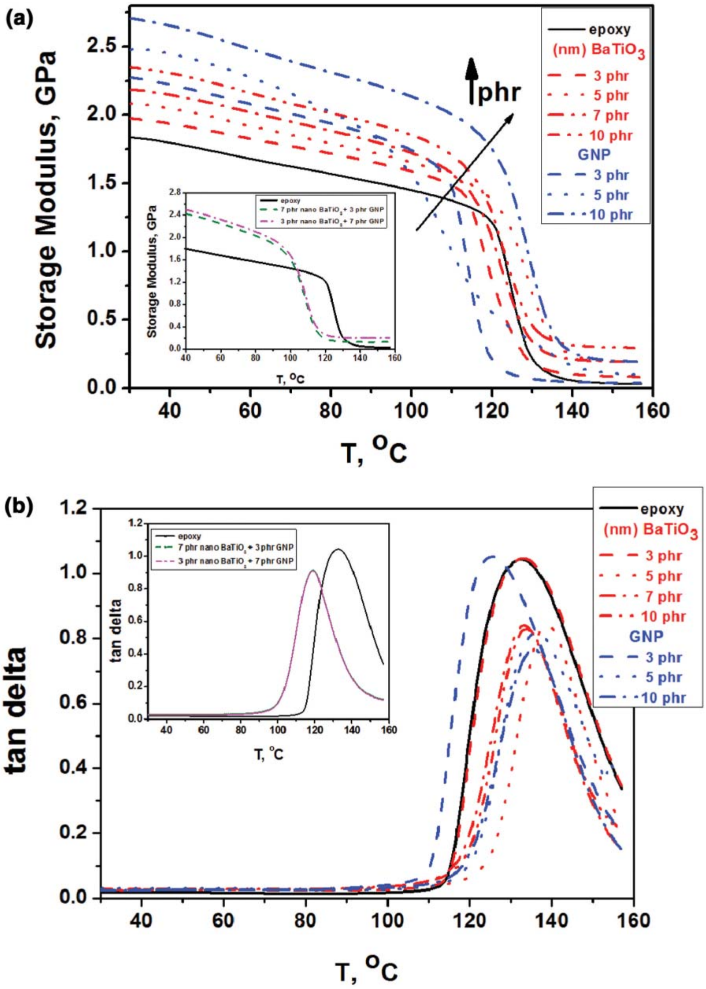

Figure 3. (a) Storage modulus and (b) loss tangent delta as a function of temperature, at $f = 1$ Hz, of all $BaTiO_3$/epoxy and GNP/epoxy nanocomposites. Inset refers to the $BaTiO_3$/GNP/epoxy hybrid systems.

micro-$BaTiO_3$/epoxy hybrid composites. The above-mentioned general trends of glass-to-rubber transition, dissipation of energy in the transition region and the enhancement of storage modulus with filler content are also observed in Figure 4(a) and 4(b). It should be noted that micro-$BaTiO_3$ composites exhibit higher values of storage modulus from the corresponding nanocomposites at the same filler loading. However, the increased tendency of nanoparticles to form agglomerates does not allow fabricating $BaTiO_3$ nanocomposites with filler content as high as in the case of the microcomposites. Regarding the micro/nano hybrid $BaTiO_3$/epoxy composites, the specimen with the higher microparticles content has increased storage modulus values. Furthermore, from the comparison of all composite systems with 10 phr filler content (Figures 3 and 4), either binary or hybrid, it is apparent that the 10 phr GNP/epoxy system attains the highest values of storage modulus.

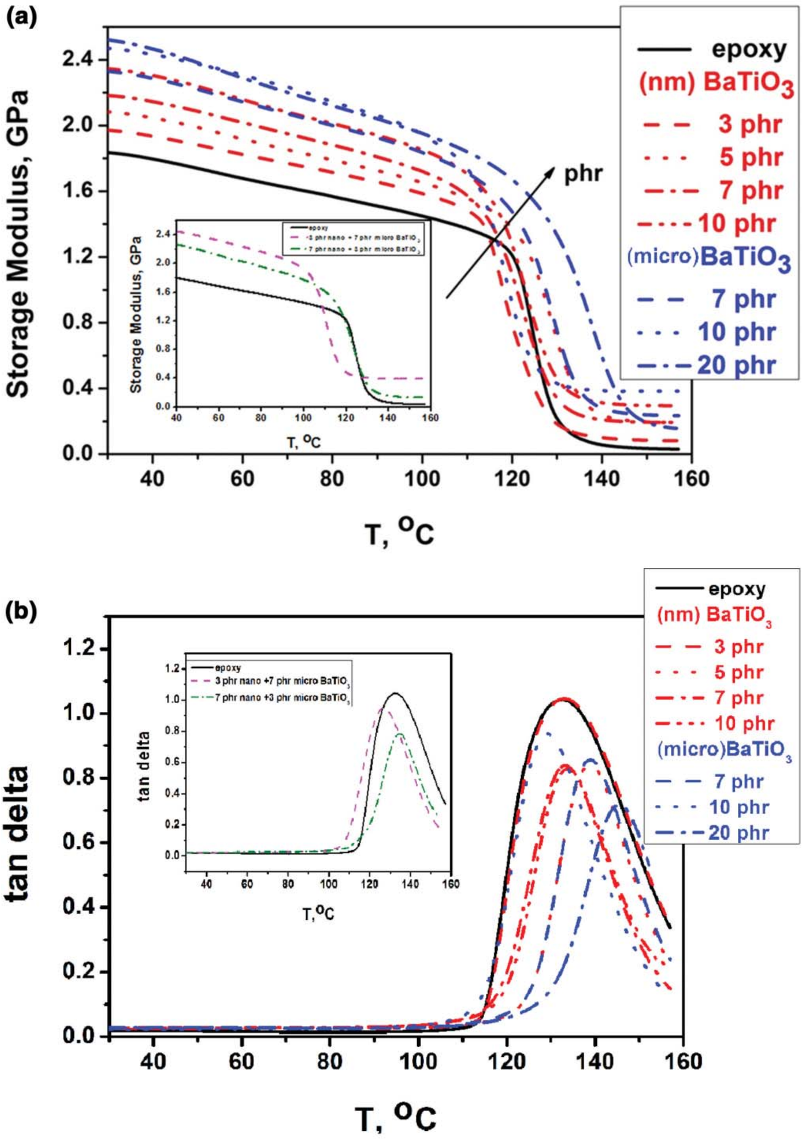

Figure 4. (a) Storage modulus and (b) loss tangent delta as a function of temperature, at $f = 1$ Hz, of the micro- and nano-$BaTiO_3$/epoxy composites. Inset refers to the micro-$BaTiO_3$/nano-$BaTiO_3$/epoxy hybrid systems.

Results from static mechanical tests, of all studied systems at ambient temperature, are depicted in Figure 5. Flexural modulus increases with filler content, being in accordance with the DMA results. At the same nano filler content, the GNP/epoxy composites exhibit higher values of flexural modulus (see Figure 5(a)). Best performance is observed for the composite with the highest GNP loading. On the other hand, in the case of $BaTiO_3$ micro, nano or hybrid micro/nano composites, at constant filler content, the 10 phr micro-particles composite displays the relative highest value of flexural modulus (see Figure 5(b)).

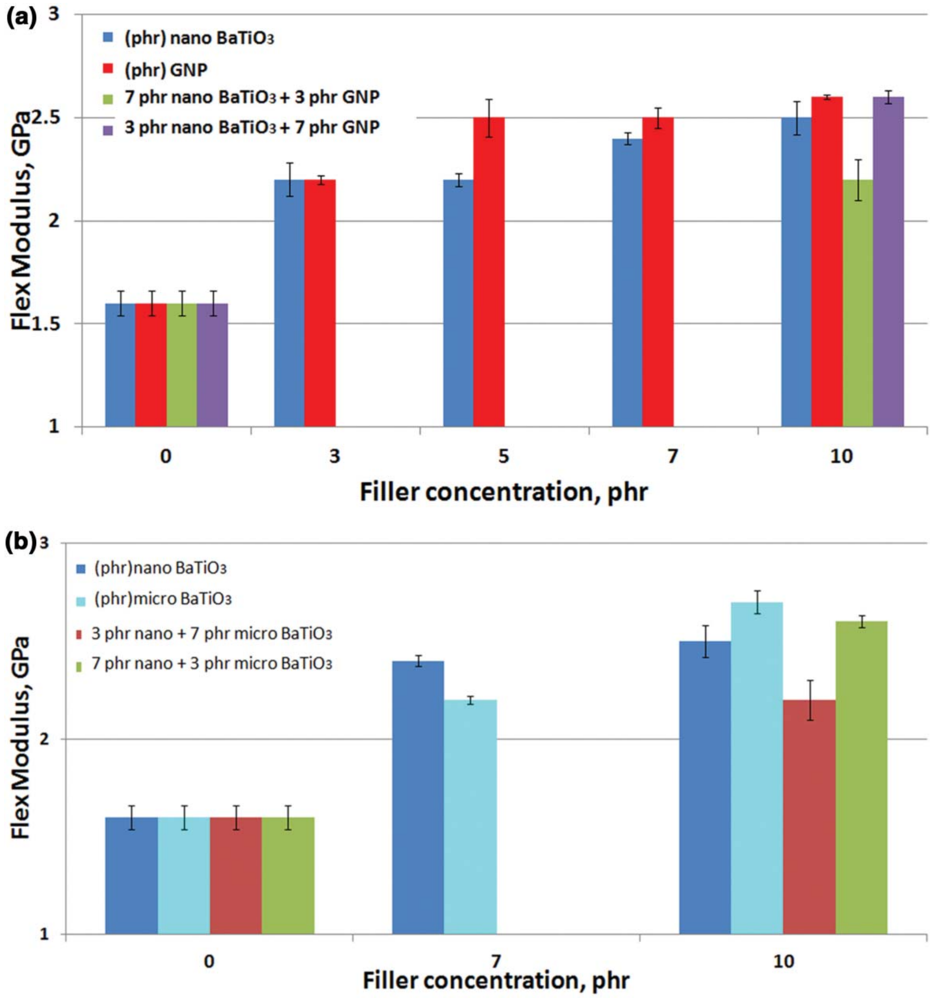

Figure 5. Flexural modulus as a function of filler content for (a) neat epoxy, $BaTiO_3$/epoxy, GNP/epoxy and $BaTiO_3$/GNP/epoxy nanocomposites, and (b) micro-$BaTiO_3$/epoxy, nano-$BaTiO_3$/epoxy and micro-$BaTiO_3$/nano-$BaTiO_3$/epoxy composites.

Dielectric data can be analysed in terms of different formalisms, such as dielectric permittivity, electric modulus or ac conductivity. Each formalism describes the same electrical phenomena occurring in the examined materials; however, under specific conditions, one could be proven more effective in extracting information for the physical mechanisms of the recorded phenomena.[19–23] In this study, dielectric data are analysed by means of both dielectric permittivity and electric modulus formalisms. Electric modulus is defined as the reverse quantity of the complex dielectric permittivity:

$$M^{*}=\frac{1}{\varepsilon^{*}}=M'+iM''=\frac{\varepsilon'}{\varepsilon'^{2}+\varepsilon''^{2}}+i\frac{\varepsilon''}{\varepsilon'^{2}+\varepsilon''^{2}}, \tag{1}$$

where ε', ε'' and M', M'' are the real and imaginary parts of dielectric permittivity and electric modulus, respectively.

Figure 6 presents a three-dimensional plots of the real (M', Figure 6(a)) and imaginary parts (M'', Figure 6(b)) of electric modulus as a function of the frequency of the applied field and temperature for the 5 phr GNP/epoxy nanocomposite. Two 'step-like' transitions from low to high values of M' are present in its spectra. The more intensive one, recorded at temperatures higher than 100 °C, is attributed to the glass-to-rubber transition of the polymer matrix (α-relaxation). At temperatures close to T_g, large parts of polymer macromolecules acquire sufficient thermal energy in order to relax simultaneously, leading to the occurrence of a relaxation process.[24] The second and weaker transition, recorded at lower temperatures and higher frequencies, is related to local rearrangements of polar side groups of the main polymer chain (β-relaxation).[5,8] Loss modulus index (M'') spectra shown in Figure 6(b), include two dielectric relaxation peaks, which correspond to the mechanisms mentioned previously, and are recorded at the areas of the transitions. Increase of temperature shifts the loss peak position to higher frequencies, since permanent and induced dipoles obtain sufficient thermal energy in order to follow faster alternations of the applied electric field.

The dielectric response of the 5 phr $BaTiO_3$/epoxy nanocomposite is presented in Figure 7. Qualitative M' and M''spectra are similar to those of Figure 6, with α- and β-relaxations present.

The dependence of the real part of dielectric permittivity (ε') on temperature at a constant frequency $f = 0.1$ Hz for all studied nanocomposites is presented in Figure 8 (a). ε' increases with filler content in the whole temperature range. However, this behaviour is more pronounced in the case of GNP/epoxy nanocomposites. Barium titanate is a wide band gap semiconductor with dielectric permittivity much higher than that of epoxy resin; thus, it is reasonable for the values of ε' to increase with the $BaTiO_3$ content. Graphite nanoplatelets exhibit enhanced conductivity relatively to both epoxy resin and barium titanate particles. The occurring electrical heterogeneity of the nanocomposites gives rise to interfacial polarization (IP), thus enforcing permittivity values. IP is present in electrically heterogeneous systems.[19,25] Unbounded charges accumulate at the interface between matrix and filler, where they form large dipoles. The induced dipoles present a difficulty to align themselves parallel to the field when frequency is high and temperature is low. Providing sufficient time (low-frequency region) and enhanced mobility via thermal agitation (high temperatures) enables the dipoles to be oriented with the field following its slow alternation. In some cases, parts of these unbounded charges are able to migrate through the specimen, thus contributing to the overall conductivity of the system. However, the small amounts of conductive filler employed in this study and the insulating nature of the polymer matrix act as a strong restriction to this movement. Since dielectric permittivity is proportional to polarization,[6] the enhancement of IP should be reflected at higher values of ε'. This trend is shown in Figure 8 at temperatures higher than 130 °C. Additionally, close to T_g, approximately at 120 °C, the increased mobility of large parts of the polymer macromolecules contributes further to the increase of dielectric permittivity values. Figure 8(b) depicts the variation of the real part of dielectric permittivity with temperature, at a constant frequency of 0.1 Hz, for composite systems with a filler content of 10 phr. This 10 phr filler content could be either only GNP or only $BaTiO_3$, or a combination of proportions of both filler types, having the content sum equal to 10 phr. By these means is given the opportunity to directly compare the effect of different fillers upon ε' at constant filler content. Dielectric performance is improved with GNP content, and the optimum performance is shown by the specimen with the highest GNP concentration.

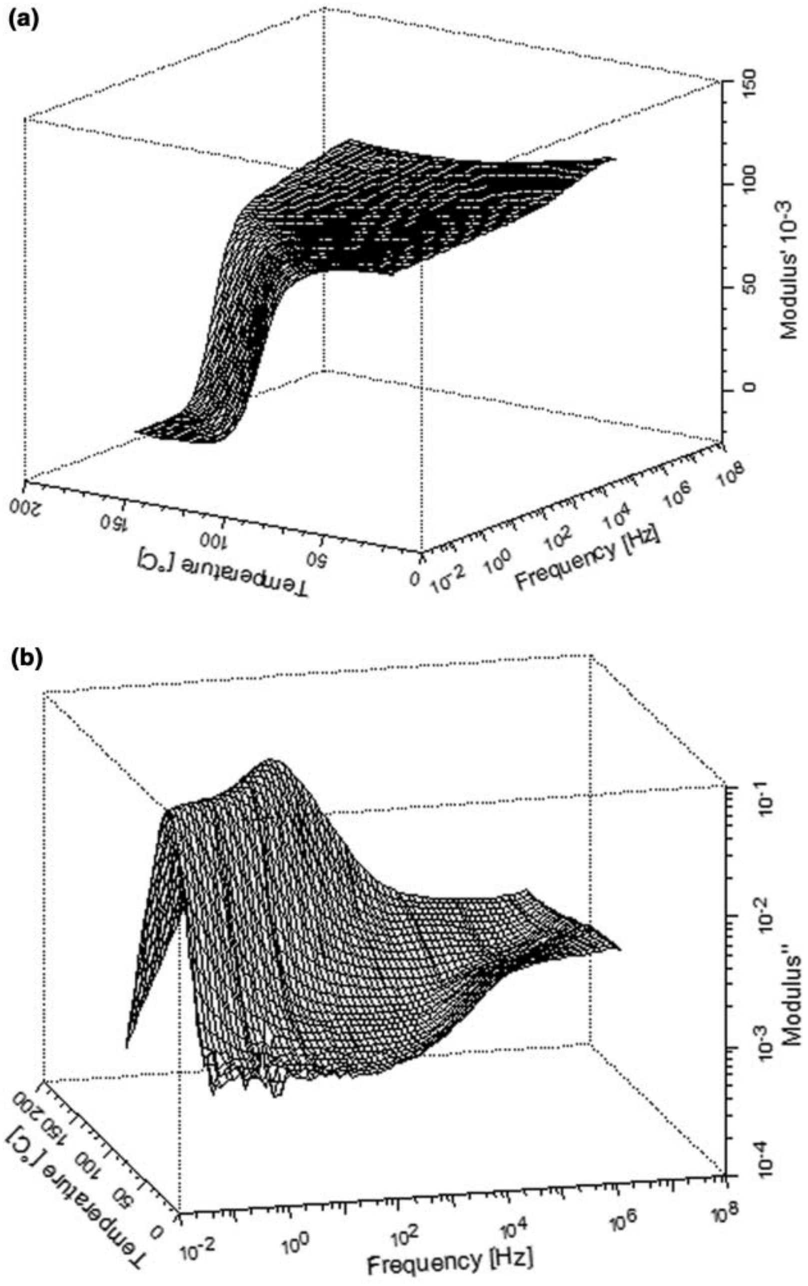

Figure 6. Real (a) and imaginary (b) part of electric modulus as a function of frequency and temperature for the 5 phr GNP/epoxy nanocomposite.

The efficiency to store energy in the examined composites is investigated via the energy density function. Energy density is determined [26,27] by

$$U = \frac{1}{2}\varepsilon_0\varepsilon' E^2, \tag{2}$$

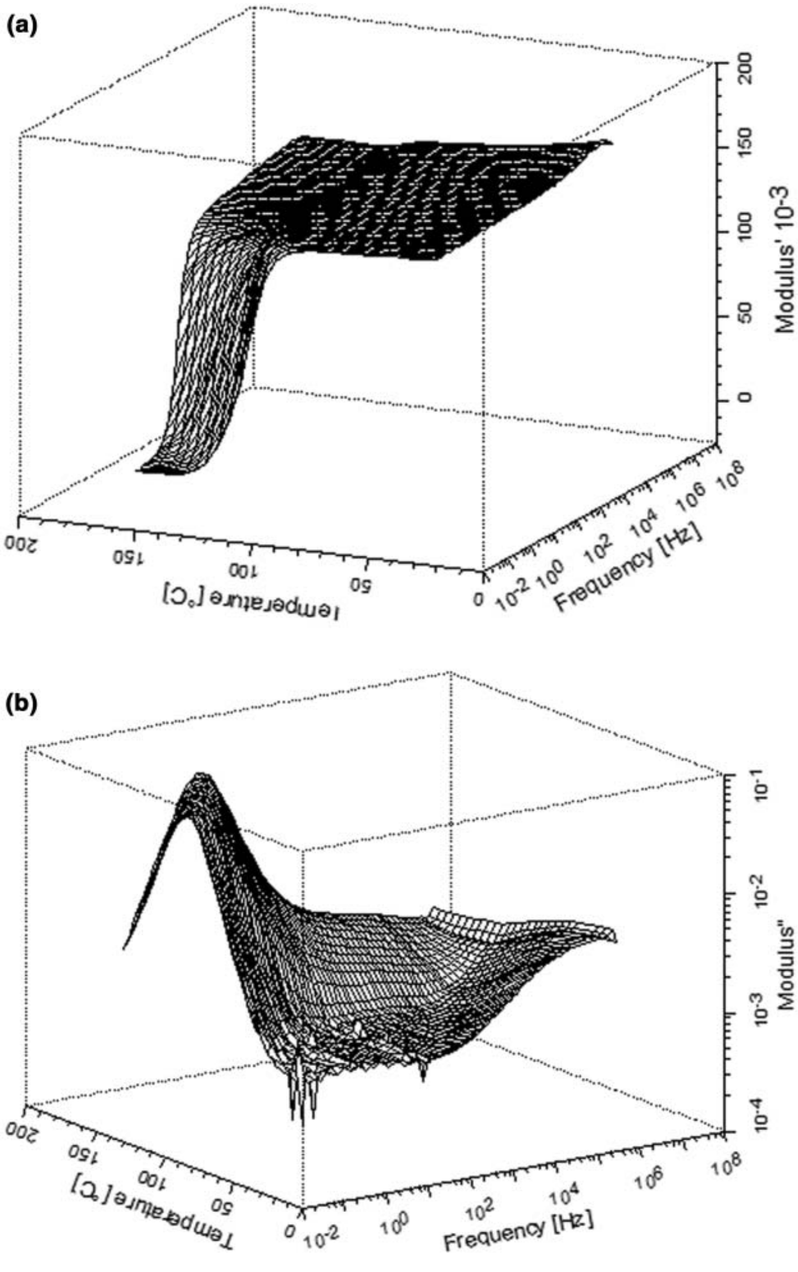

Figure 7. Real (a) and imaginary (b) part of electric modulus as a function of frequency and temperature for the 5 phr $BaTiO_3$/epoxy nanocomposite.

where ε_0 is the permittivity of fee space and E is the electric field's intensity. From Equation (2), it is evident that energy density rapidly increases with the electric field's intensity. The energy density function approaches its maximum value when the intensity of the electric field tends to the material's breakdown strength. However, below the dielectric breakdown strength, the field's intensity is an external to the material parameter and

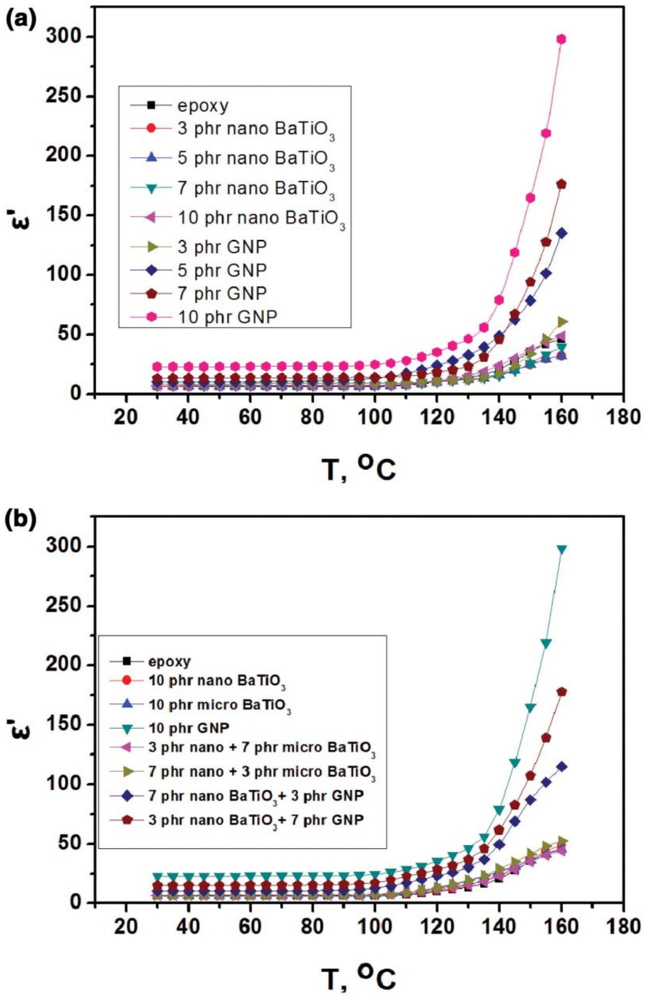

Figure 8. Real part of dielectric permittivity as a function of temperature for (a) epoxy and all $BaTiO_3$/epoxy and GNP/epoxy nanocomposites, and (b) epoxy and all examined composites with a filler content equal to 10 phr, at 0.1 Hz.

the only material property present in Equation (2) is ε'. Thus, the dependence of energy density upon the frequency of the field and the temperature should be analogous to that of dielectric permittivity. Energy density as a function of frequency, at 30 °C, for all nanocomposites with 10 phr filler content is shown in Figure 9(a). Figure 9(b) depicts the dependence of energy density on temperature, at a constant frequency of 0.1 Hz, for the same set of nanocomposites as in Figure 9(a).

In all studied cases, at a constant applied field $E = 0.5$ kV/m, energy storage increases with filler content and especially with GNP content, in the whole frequency and temperature range. The presence of GNP inclusions within the epoxy matrix increases the energy storage efficiency of the nanocomposite systems up to two orders of magnitude. Optimum behaviour is exhibited, as in the case of mechanical and dielectric performance, by the nanocomposite with the maximum GNP loading. In the literature, studies on energy storage in various nanocomposites are available. However, a direct comparison is not easy, since reported values are dependent on the applied electric field, the measuring frequency of ε', the temperature and the filler content. To keep a common denominator, it could be examined the relative increase of the stored energy between an unfilled polymer matrix and the optimum (in each case) nanocomposite at ambient temperature, at a low measuring frequency of ε', and at a constant (and preferentially not high) electric field. Under these conditions, a 10% increase of the stored energy has been reported in a 6% wt reinforced montmorillonite/epoxy system, a 15% increase for a montmorillonite/$BaTiO_3$/epoxy hybrid system, at 6% wt and 10% volume fraction loading, respectively, and an almost 33% increase in the stored energy in a 30% in volume fraction reinforced $BaTiO_3$/epoxy nanocomposite.[3] Additionally, in a $BaTiO_3$/ferroelectric polymer study, an

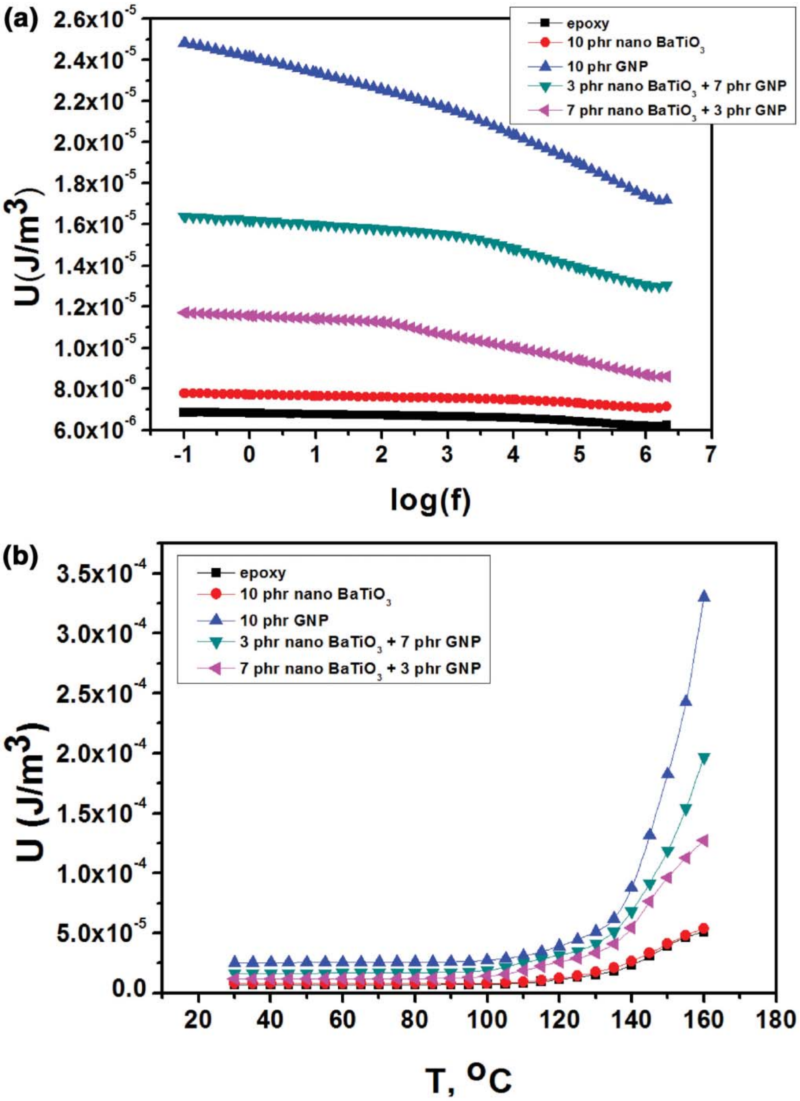

Figure 9. Energy density, at constant field, as a function of (a) frequency at 30 °C and (b) temperature at $f = 0.1$ Hz, for epoxy and all examined composites with a filler content equal to 10 phr.

increase of the stored energy of greater than 20% has been reported at maximum volume fraction loading of 30%,[28] while in a study of GNP/epoxy nanocomposites, a 40% increase of energy storage was evidenced for a 10 phr GNP/epoxy system.[18] Finally, in our case the corresponding increase varies between almost 10% and 40%.

4. Conclusions

Micro- and/or nano-$BaTiO_3$/epoxy composites as well as GNP/epoxy resin and GNP/$BaTiO_3$/epoxy nanocomposites were prepared and studied by varying the type and the amount of the filler content. SEM images of the prepared systems reveal that the dispersion of graphite nanoplatelets and barium titanate nanoparticles can be considered as satisfactory. XRD spectra of the composites include characteristic peaks from GNP and $BaTiO_3$ particles. The mechanical performance of the systems is improved with GNP content under both static and dynamic loading. Dielectric permittivity increases with filler content and temperature, especially in the case of GNP inclusions, and diminishes rapidly with frequency. At least two relaxation processes have been recorded in all studied systems. They are attributed to glass-to-rubber transition (α-mode) and re-arrangement of polar side groups (β-mode). Finally, the addition of GNP and/or $BaTiO_3$ nanoinclusions into epoxy increases the ability of the material to store energy. The effect is more pronounced in the case of the GNP nanocomposites.

Funding

This research has been co-financed by the European Union (European Social Fund – ESF) and Greek national funds through the Operational Program 'Education and Lifelong Learning' of the National Strategic Reference Framework (NSRF) – Research Funding Program: THALES [grant number MIS 379346].

References

[1] Psarras GC. Nanodielectrics: an emerging sector of polymer nanocomposites. Express Polym Lett. 2008;2:460.
[2] Dang Z-M, Yu Y-F, Xu H-P, Bai J. Study on microstructure and dielectric property of the $BaTiO_3$/epoxy resin composites. Compos Sci Technol. 2008;68:171–178.
[3] Toner V, Polizos G, Manias E, Randal CA. Epoxy-based nanocomposites for electrical energy storage. I: effects of montmorillonite and barium titanate nanofillers. J Appl Phys. 2012;108:074116.
[4] Ramajo L, Reboredo MM, Castro MS. $BaTiO_3$-epoxy composites for electronic application. Int J Appl Ceram Technol. 2010;7:444–451.
[5] Patsidis AC, Kalaitzidou K, Psarras GC. Dielectric response, functionality and energy storage in epoxy nanocomposites: barium titanate vs exfoliated graphite nanoplatelets. Mater Chem Phys. 2012;135:798–805.
[6] Patsidis A, Psarras GC. Dielectric behaviour and functionality of polymer matrix – ceramic $BaTiO_3$ composites. Express Polym Lett. 2008;4:718–726.
[7] Kumar N, Nath R. Experimental studies for stability of ferroelectric phase in potassium nitrate composite films. Polym Eng Sci. 2013;53:1856–1863.
[8] Patsidis AC, Kalaitzidou K, Psarras GC. Carbon or barium titanate reinforced epoxy resin nanocomposites: dielectric, thermomechanical and functional behavior. J Adv Phys. 2013;2:7–12.
[9] Patsidis AC, Psarras GC. Structural transition, dielectric properties and functionality in epoxy resin – barium titanate nanocomposites. Smart Mater Struct. 2013;22:115006.
[10] Parthenios J, Psarras GC, Galiotis C. Adaptive composites incorporating shape memory alloy wires. Part 2: development of internal recovery stresses as a function of activation temperature. Compos Part A. 2001;32:1735–1747.

[11] Petalis P, Makris N, Psarras GC. Investigation of the phase transformation behaviour of constrained shape memory alloy wires. J Therm Anal Calorim. 2006;84:219−224.

[12] Psarras GC. Smart polymer systems: a journey from imagination to applications. Express Polym Lett. 2011;5:1027.

[13] Psarras GC, Sofos GA, Vradis A, Anastassopoulos DL, Georga SN, Krontiras CA, Karger-Kocsis J. HNBR and its MWCNT reinforced nanocomposites: crystalline morphology and electrical response. Eur Polym J. 2014;54:190−199.

[14] Cao A, Xu C, Liang J, Wu D, Wei B. X-ray diffraction characterization on the alignment degree of carbon nanotubes. Chem Phys Lett. 2001;344:13−17.

[15] Li W, Liang C, Zhou W, Qiu J, Zhou Z, Sun G, Xin Q. Preparation and characterization of multiwalled carbon nanotube-supported platinum for cathode catalysts of direct methanol fuel cells. J Phys Chem B. 2003;107:6292−6299.

[16] Psarras GC. Charge transport properties in carbon black/polymer composites. J Polym Sci Part B. 2007;45:2535−2545.

[17] Ioannou G, Patsidis A, Psarras GC. Dielectric and functional properties of polymer matrix/ZnO/$BaTiO_3$ hybrid composites. Compos Part A. 2011;42:104−110.

[18] Patsidis AC, Kalaitzidou K, Psarras GC. Graphite nanoplatelets/polymer nanocomposites: thermomechanical, dielectric, and functional behaviour. J Therm Anal Calorim. 2014;116:41−49.

[19] Tsangaris GM, Psarras GC, Kouloumbi N. Electric modulus and interfacial polarization in composite polymeric systems. J Mater Sci. 1998;33:2027−2037.

[20] Kontos GA, Soulintzis AL, Karahaliou PK, Psarras GC, Georga SN, Krontiras CA, Pisanias MN. Electrical relaxation dynamics in TiO_2-polymermatrix composites. Express Polym Lett. 2007;1:781−789.

[21] Psarras GC, Gatos KG, Karahaliou PK, Georga SN, Krontiras CA, Karger-Kocsis J. Relaxation phenomena in rubber/layered silicate nanocomposites. Express Polym Lett. 2007;1:837−845.

[22] Hernandez M, Carretero-Gonzalez J, Verdejo R, Ezquerra TA, Lopez-Manchado MA. Molecular dynamics of natural rubber/layered silicate nanocomposites as studied by dielectric relaxation spectroscopy. Macromolecules. 2010;43:643−651.

[23] Psarras GC, Siengchin S, Karahaliou PK, Georga SN, Krontiras CA, Karger-Kocsis J. Dielectric relaxation phenomena and dynamics in polyoxymethylene/ polyurethane/alumina hybrid nanocomposites. Polym Int. 2011;60:1715−1721.

[24] Psarras GC. Conductivity and dielectric characterization of polymer nanocomposites. In: Tjong SC, Mai YM editors. Polymer nanocomposites: physical properties and applications. Cambridge: Woodhead Publishing Limited; 2010. p. 31−69.

[25] Kalini A, Gatos KG, Karahaliou PK, Georga SN, Krontiras CA, Psarras GA. Probing the dielectric response of polyurethane/alumina nanocomposites. J Polym Sci Part B. 2010;48:2346−2354.

[26] Wang Q, Zhu L. Polymer nanocomposites for electrical energy storage. J Polym Sci Part B. 2011;49:1421−1429.

[27] Dang Z-M, Yuan J-K, Zha J-W, Zhou T, Li S-T, Hu G-H. Fundamentals, processes and applications of high-permittivity polymer-matrix composites. Prog Mater Sci. 2012;57:660−723.

[28] Li J, Claude J, Norena-Franco LE, Seok SI, Wang Q. Electrical energy storage in ferroelectric polymer nanocomposites containing surface-functionalized $BaTiO_3$ nanoparticles. Chem Mater. 2008;20:6304−6306.